Contents lists available at ScienceDirect

Ceramics International

journal homepage: www.elsevier.com/locate/ceramint

A facile, time-saving fabrication method of high purity $CsPbBr_3$ films for efficient solar cells

Guoshuai Zhang [a,b], Xiaobing Cao [a,**], Jinquan Wei [c,***], Jinpeng Li [b,*]

[a] School of Applied Physics and Materials, Wuyi University, Jiangmen, Guangdong, 529020, PR China
[b] Key Laboratory of Luminescence and Optical Information, Ministry of Education, School of Physical Science and Engineering, Beijing Jiaotong University, Beijing, 100044, China
[c] State Key Lab of New Ceramics and Fine Processing, Education Ministry Key Laboratory for Advanced Materials Processing Technology, School of Materials Science and Engineering, Tsinghua University, Beijing, 100084, China

ARTICLE INFO

Handling Editor: P. Vincenzini

Keywords:
Two-step method
Solution process
$CsPbBr_3$ perovskite
Solar cells

ABSTRACT

All-brominated cesium lead bromide ($CsPbBr_3$) perovskite solar cells (PSCs) have drawn growing attention owing to unprecedented stability in the family of perovskites. It usually employs a two-step method to prepare $CsPbBr_3$ films owing to the low solubility of CsBr in the common solvents. The researchers have to provide enough Cs source through increasing the reaction time or repeat times of CsBr deposition so as to obtain the target $CsPbBr_3$ films. The long preparation period and tedious process increase the time and economic cost, which may limit the practical application of $CsPbBr_3$ solar cells. Herein, a facile method is proposed to prepare $CsPbBr_3$ films, in which appropriate CsBr is pre-introduced into $PbBr_2$ solutions in the first step, and CsBr/2-methoxyethanol solution (~35 mg mL^{-1}) is used as solution conversion medium in the second step. Benefitting from the pre-introduction of CsBr in the first step, a single phase of $CsPbBr_3$ films with full coverage can be conversed for only once CsBr supplementation. After integrating the $CsPbBr_3$ films into a solar cell, it delivers a power conversion efficiency (PCE) of 7.48% basing on the configuration of FTO/TiO_2/$CsPbBr_3$/Carbon. This work largely shortens the preparation time of $CsPbBr_3$ films, which may provide a practical way for the large-scale production of $CsPbBr_3$ based devices.

1. Introduction

All-inorganic perovskite $CsPbBr_3$ attracts more attentions in optoelectronic devices such as solar cells, photodetectors and light-emitting devices, due to its superior optoelectronic properties and high stability in air conditions. The highly compatible with the carbon electrode in ambient condition makes $CsPbBr_3$ as a reasonable candidate to full solution-processed solar cell fabrication [1–4]. The big challenge to $CsPbBr_3$ films for solar cells is to fabricate pure and smooth thick perovskite layer due to the poor solubility of CsBr in traditional organic solvents. The common way is so-called two-step method, in which $PbBr_2$ films were firstly prepared, and then exposed to CsBr methanol solution for an optimized time, usually at least 10 min, to obtain desired $CsPbBr_3$ films [1–8]. However, the reaction time is so sensitive that either too short or too long reaction time could generate byproducts like $CsPb_2Br_5$ and Cs_4PbBr_6, which limits the photovoltaic performance and lead to other side effects [9–11].

To exclude the byproducts, Duan et al. [12] proposed a multi-steps solution processed technique to prepare high purity $CsPbBr_3$ films. In this method, a drop of CsBr/methanol was spin-coated onto the $PbBr_2$ films, followed by annealing at 250 °C for 5 min, then repeated this process for several cycles. According to their report, the components, crystal structure, and morphology of the as-prepared perovskite films are strongly dependent on the preparation cycles. Especially, it needs at least four cycles which cost no less than 20 min to obtain pure $CsPbBr_3$ films in their method. Obviously, it is a time-consuming method to prepare pure phase $CsPbBr_3$ films. Meanwhile, the methanol used to dissolve CsBr could decompose $CsPbBr_3$ during the treatment, which may resulting in poor morphology and more defects in the final products [13]. In order to eliminate methanol as the solvent, Feng et al. replaced

* Corresponding author.
** Corresponding author.
*** Corresponding author.
E-mail addresses: caoxb14@tsinghua.org.cn (X. Cao), jqwei@tsinghua.edu.cn (J. Wei), jinpengli@bjtu.edu.cn (J. Li).

https://doi.org/10.1016/j.ceramint.2023.03.279
Received 26 January 2023; Received in revised form 18 March 2023; Accepted 28 March 2023
Available online 31 March 2023

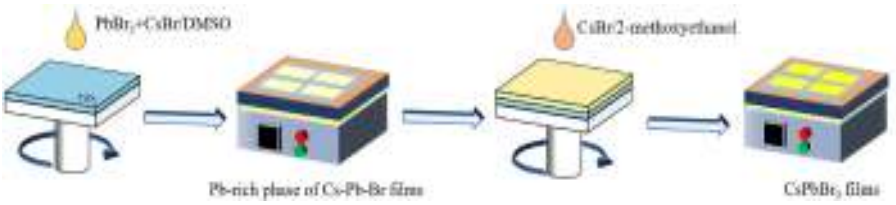

Scheme 1. Schematic illustration of the deposition processes of $CsPbBr_3$ films.

Fig. 1. The photograph of solutions with different molar ration between $PbBr_2$ and CsBr in DMSO. (a)2:0; (b) 2:0.5; (c) 2:1; (d) 2:1.5.

the methanol with 2-methoxyethanol for preparing CsBr solution [9]. They can obtain single phase $CsPbBr_3$ film in a few minutes. However, the morphology of this film is too poor to use in solar cell devices. Sooner after, they proposed a binary solvent system of 2-methoxyethanol/isopropanol to prepare CsBr solution (~15 mg mL^{-1}), and then simultaneously optimized the morphology and phase of the target $CsPbBr_3$ film by dipping the $PbBr_2$ into the CsBr/(2-methoxyethanol + isopropanol) solution for 40 min, and a power conversion efficiency (PCE) of 7.29% was achieved basing on FTO/TiO_2/$CsPbBr_3$/Carbon architecture [14]. Recently, Chen et al. also employed 2-methoxyethanol solvent for dissolving CsBr to yield high-quality $CsPbBr_3$ films and obtained PCE of 6.54%, but they still need to use multi-steps solution processed method [15]. Evidently, the poor solubility of CsBr in common solvents lead to complicated fabrication processes and long crystallization period.

By reviewing the previous report, these processes usually separate $PbBr_2$ solution with CsBr solution. Whether separating certain amount of CsBr into both poor and favourable solvents could reduce the preparation time needs to be further investigated. In this work, appropriate CsBr is introduced into $PbBr_2$/DMSO solution in the first step to prepare Pb-rich phase of Cs–Pb–Br films. Then, high quality $CsPbBr_3$ films are obtained by spin-coating a CsBr/2-methoxyethanol (~35 mg mL^{-1}) onto the Cs–Pb–Br films for only once. As a consequence, a hole transport layer (HTL) free $CsPbBr_3$ perovskite solar cell by using carbon act as the electrode shows a PCE of 7.48%, and possesses excellent stability in the air atmosphere. This work provides a facile and cost-effective approach to prepare $CsPbBr_3$ films, making it a promising application for $CsPbBr_3$ based devices.

2. Experiment methods

Device fabrication: Fluorine-doped tin oxide (FTO) glass substrates were cleaned by sonication in deionized water, 2-propanol, ethanol, and deionized water successively. The deposition of electron transport layer of TiO_2 films are achieved according to our previous work [16].

The perovskite films were fabricated by a two-steps spin-coating technology, as shown in Scheme 1. In the first step, the matrices were prepared from $PbBr_2$/DMSO solution (~2.0 M) with addition of different molar ratios of CsBr to form perovskite precursor solutions. Before the deposition of perovskite films, all precursor solutions were filtered using 0.45 μm pore size filter and immediately used. Then, the different solutions were spin-coated onto pre-heated substrates 80 °C at

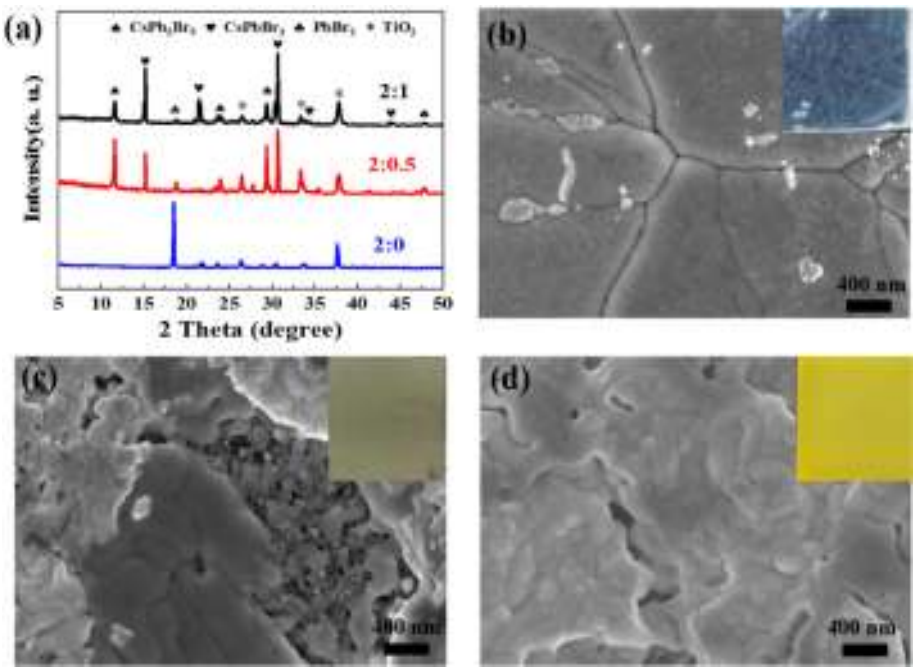

Fig. 2. (a) XRD curves of the films prepared from different solutions. Surface SEM images of the films prepared from different solution in the first step. (b) 2:0; (c) 2:0.5; (d) 2:1. The inset are the photograph of corresponding the films.

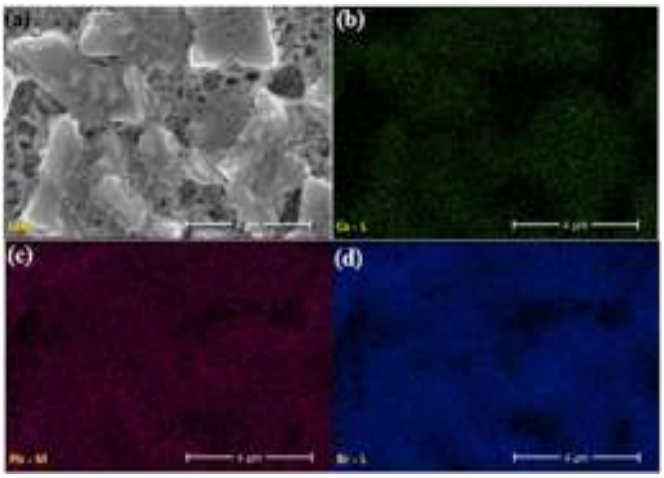

Fig. 3. (a) The SEM image of EDX result of the Cs–Pb–Br film prepared from the solution of 2:1; The mapping of the film elements, (b) Cs; (c) Pb; (d) Br.

a speed of 3000 rpm for 30 s, followed by an anneal treatment at 100 °C for 5 min in a N_2-filled glovebox. In the second step, 90 μL CsBr/2-methoxyethanol solution (~35 mg mL^{-1}) (see Fig. S1) was dropped on the matrices and stay it for 60 s, then the substrates were spin-coated at 2000 rpm for 30 s in ambient air atmosphere. The matrices are further annealed at 250 °C for 5 min to form Cs–Pb–Br films. Finally, the carbon electrode was deposited by using screen printing of carbon paste with drying at 100 °C for 10 min.

Characterization: The phase and morphology of $PbBr_2$ and Cs–Pb–Br films were measured by X-ray diffraction (PANalytical X'Pert[3] Powder) and field-emission scanning electron microscopy (NovaTM NanoSEM 430), respectively. The UV-Vis spectrophotometer (Shimazu UV-2550) was employed to get the absorption spectra of the $PbBr_2$ and Cs–Pb–Br films. A photoluminescence spectrometer (Edinburgh Instruments, LP 980) was utilized to obtain the photoluminescence (PL) spectra. The photovoltaic performance of solar cells was recorded using a Keithley 2400 under AM 1.5G simulated solar illumination. The incident photo-to-current collection efficiency spectrum (IPCE) of solar cells were performed an integrated system from Enlitech (QE-R3011).

3. Results and discussion

We first investigated the solubility of CsBr in $PbBr_2$/DMSO solution. As shown in Fig. 1, it is still a clear solution even the concentration of CsBr increases from 0 M to 1.0 M in the mixtures (Fig. 1a–c). However, the mixture becomes turbid when the concentration of CsBr increases to 1.5 M (Fig. 1d). In light of the dissolution state, we employ the solutions composed of different molar ratios between $PbBr_2$ and CsBr from 2:0, 2:0.5 and 2:1 to prepare the Cs–Pb–Br matrices in the first step for understanding the phase composition.

The as-prepared samples are examined by the X-ray diffraction (XRD). Fig. 2a shows the XRD patterns of the films prepared from

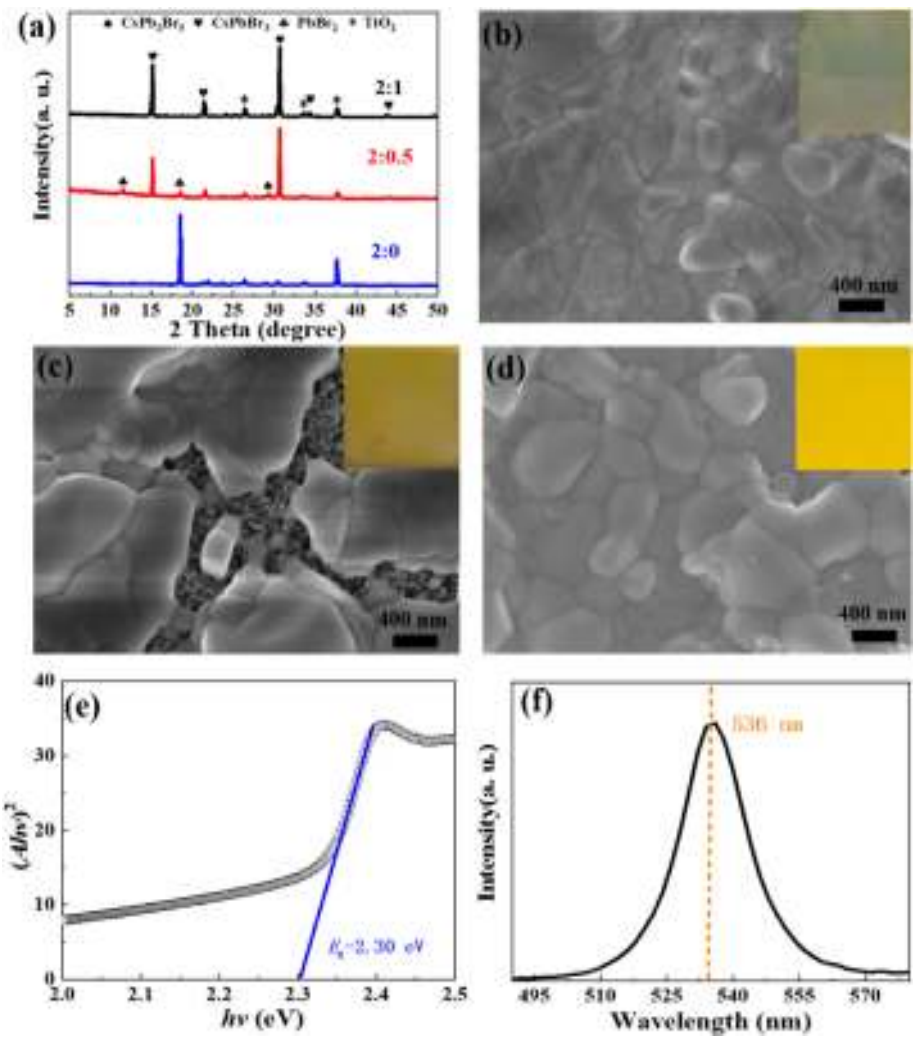

Fig. 4. (a) The normalized XRD curves of the Cs–Pb–Br films prepared from different solutions; Surface SEM images of Cs–Pb–Br films from different solutions; (b) 2:0; (c) 2:0.5; (d) 2:1. (e) $(Ahv)^2$-hv curve obtained from the UV absorption spectrum, and (f) the steady PL spectrum of the Cs–Pb–Br films film prepared from the solution of 2:1. The inset are the photograph of corresponding the Cs–Pb–Br films.

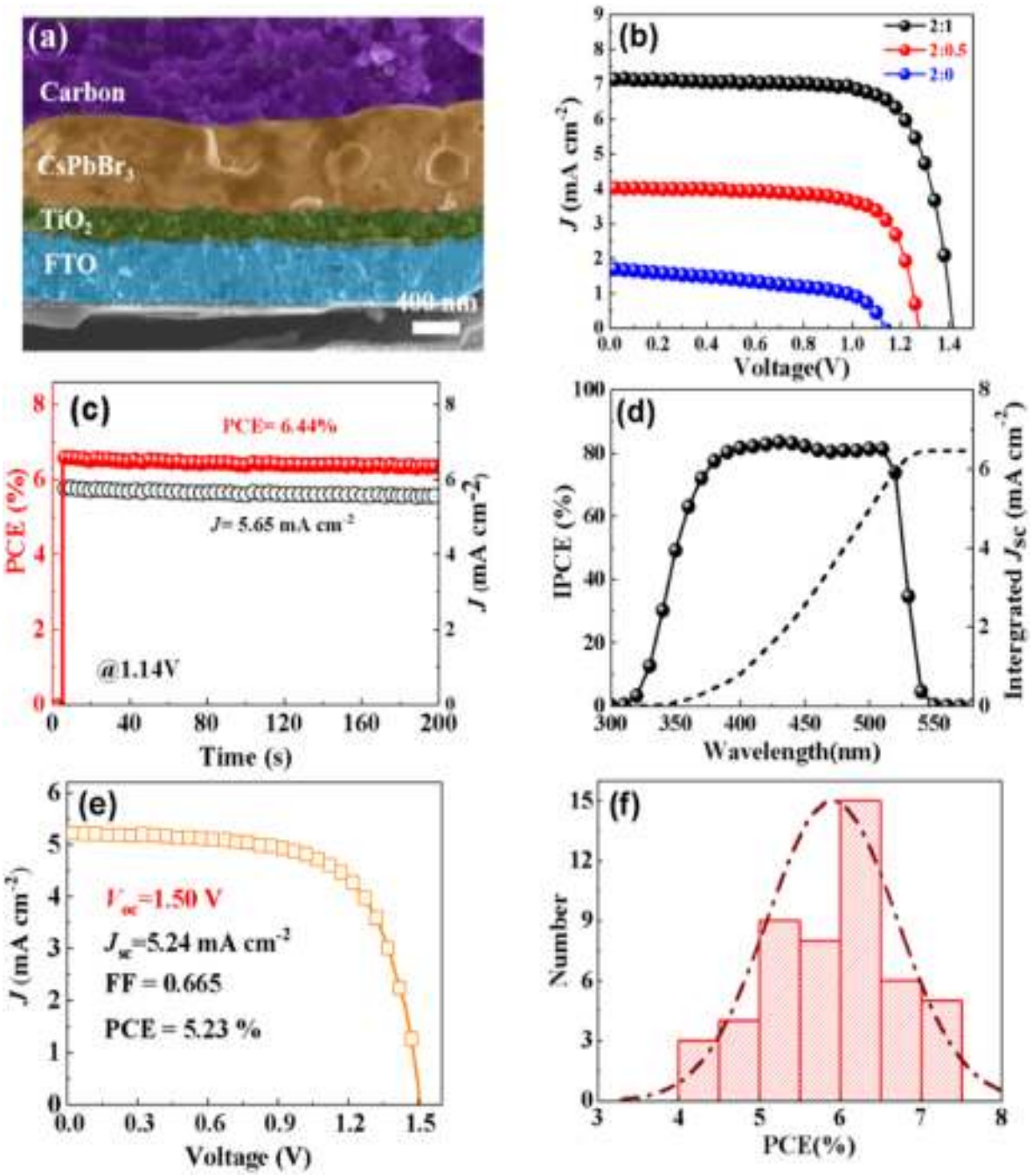

Fig. 5. (a) The device configuration of solar cells; (b) *J-V* curves of the best PSCs prepared from different solutions; (c) the steady output of best solar cells by applying a voltage at the maximum output point. (d) IPCE spectrum; (e) the *J-V* curves having highest V_{oc}; (f) the distribution of PCE from a series of solar cells.

Table 1
The photovoltaic performance of best solar cells prepared from different solutions.

Solution	V_{oc}(V)	J_{sc}(mA cm^{-2})	FF(%)	PCE(%)
2 : 0	1.13	1.70	51.84	0.99
2 : 0.5	1.27	4.02	73.05	3.73
2 : 1	1.41	7.15	74.07	7.48

different solutions. The film prepared from the solution of 2:0 are pure $PbBr_2$, which is confirmed by the characteristic peak at 18.5° corresponding to the (020) crystal plane [17]. In addition to having $PbBr_2$ in the film when 0.5 M CsBr is introduced into the solution, the obvious diffraction peaks can be indexed at 15.2°, 21.6°, 30.7°, 34.3° and 44.1° correspond to the (100), (110), (200), (210) and (220) planes of the $CsPbBr_3$ phase, respectively. Moreover, the film still shows the peaks at 11.7°, 23.4° , 29.4° and 47.9° correspond to the (002), (210), (213) and (420) planes of the $CsPb_2Br_5$ respectively [18], indicating the coexistence of $CsPb_2Br_5$, $CsPbBr_3$ and $PbBr_2$ in the Cs–Pb–Br films. When the concentration increased to 1.0 M, the $CsPbBr_3$ component increases in accompanied with the decreases of $PbBr_2$ and $CsPb_2Br_5$. We also study the surface morphology evolution by using scanning electron microscopy (SEM). Fig. 2b shows a SEM image of film prepared by pure $PbBr_2$ solution. The film exhibits an extremely smooth morphology with dense and compact structure, which is not beneficial for the permeation of CsBr solution in further step treatment. When including CsBr into the solution, the as-prepared films become much rougher with many pores and cracks on the surface (Fig. 2c and d). These rough morphologies have significant impacts on the permeation of CsBr/2-methoxyethanol solution in the second step treatment [19,20]. As shown in the insets of Fig. 2, the colours of the films evolves from transparent (Fig. 2b inset) to light yellow (Fig. 2d inset) when the films prepared from the solution

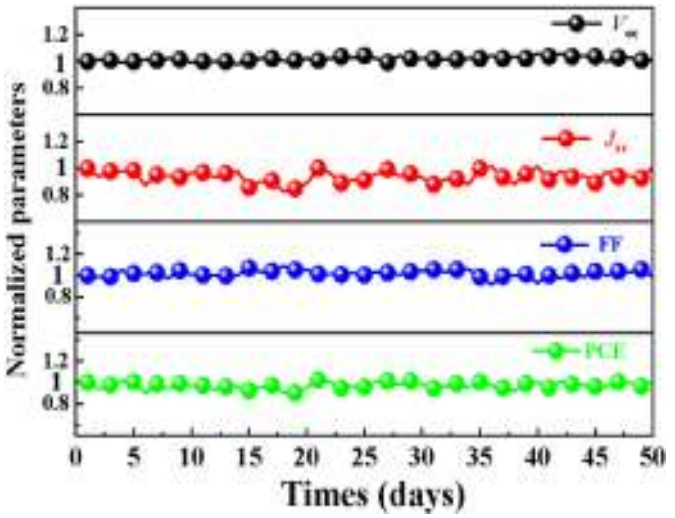

Fig. 6. The evolution of normalized parameters of solar cell at air atmosphere with temperature of ~30 °C and relative humidity of ~45%.

of 2:1, which is close to the intrinsic yellow of the $CsPbBr_3$ films. The UV/Vis absorption spectra of the films (see Fig. S2) also confirm the existence of $CsPbBr_3$ in the films, which is evidenced by an absorbance onset near 530 nm, corresponding to the bandgap of ~2.32 eV for $CsPbBr_3$ [21].

In order to learn the elements distribution in the films, we perform the energy-dispersive X-ray spectroscopy (EDX) experiments on the films prepared from the solution of 2:1 (Fig. S3). Besides the element from the substrates (Ti and O), Cs, Pb and Br element are also detected in the films, showing the existence of Cs in the films. These results strongly demonstrate that the element of Cs and Br are successfully introduced into the films. Fig. 3b–d are the elemental mapping of Cs, Pb and Br in the films, showing a uniform distribution of those elements in the films. Combined with the elemental ratio of EDX data (see Table S1), it is found that Cs:Pb:Br is close to 1:2:5 coincided with elemental ratio of the precursor solution of 2:1. Those results demonstrate that it is an effective way to supply the Cs source by introducing CsBr into the $PbBr_2$ solution in our first step treatment.

Fig. 4a is the normalized XRD curves of the Cs–Pb–Br films prepared from different solutions after reacting with CsBr/2-methoxyethanol solution, followed by an annealing treatment. Some $PbBr_2$ are still remained in the Cs–Pb–Br films prepared from the solution of 2:0. There are very weak diffraction peaks of $CsPbBr_3$ in the XRD pattern (blue line in Fig. 4a), indicating a tiny amount of $CsPbBr_3$ exists in the films due to Cs element deficiency. The phase of $CsPbBr_3$ begins to dominate in the Cs–Pb–Br films when 0.5 M CsBr is introduced into the $PbBr_2$ solution in the first step, but still exists $PbBr_2$-riched $CsPb_2Br_5$ phase in the film (red line in Fig. 4a). Therefore, it is necessary to supply Cs source so as to obtain single phase $CsPbBr_3$ films. As expected, it produces pure $CsPbBr_3$ films when 1.0 M CsBr is added to the $PbBr_2$ solution (dark line in Fig. 4a). By checking with EDX analysis (see Fig. S4 and Table S2), it is found that Cs, Pb and Br are uniform distributed and the ratio is close to 1:1:3. Those results demonstrate that it is an effective way to get pure phase $CsPbBr_3$. Fig. 4b to d show the morphology and related photos (inset figures) of the Cs–Pb–Br films after second step treatment. For the Cs–Pb–Br films prepared from the solution of 2:0, there are some small grains on the surface, which is different from the $PbBr_2$ films prepared in the first step (Fig. 2b). These small grains may be $CsPbBr_3$ grains, which is evidenced by the yellow dots on the films. There are apparent cracks in the Cs–Pb–Br films fabricated from the solution of 2:0.5 (Fig. 4c), which is consistent with the morphology of the mother matrix in the first step (Fig. 2c). The cracks in the Cs–Pb–Br films can act as the current-shunting pathways, leading to a serious current leakage and recombination loss [22–24]. Meanwhile, the film exhibits nonuniform yellow color. In contrast, matrix prepared from the solution of 2:1 exhibits fully covered morphology, this feature is further confirmed in large scale SEM image of this film (Fig. S5). The photograph of the $CsPbBr_3$ film also exhibits uniform yellow color, demonstrating a uniform feature in a large scale. The UV–vis absorption spectrum of the Cs–Pb–Br film prepared from the solution of 2:1 shows an onset at ~530 nm (Fig. S6). Fig. 4e shows the Tauc plot of the film prepared from the solution of 2:1. The optical bandgap (E_g) is fitted to be ~2.3 eV, which is consistent with previous reports [10,25,26]. The characteristic bandgap of $CsPbBr_3$ can also be demonstrated by the steady PL spectrum (Fig. 4f), which shows an emission peak at ~536 nm, corresponding to an optical bandgap of ~2.3 eV. These results demonstrate that our method is an effective way to prepare high-purity $CsPbBr_3$ films through pre-introducing appropriate CsBr into $PbBr_2$ solution.

To examine the film performance in a full solution-processed device structure, we construct an HTL-free solar cell with a configuration of FTO/TiO_2/$CsPbBr_3$/Carbon. Fig. 5a presents a cross-sectional SEM image of a solar cell sample, in which the $CsPbBr_3$ films are prepared from the solution of 2:1. It clearly indicates that the $CsPbBr_3$ grains are large enough to occupy the whole thickness of ~600 nm in active layer with dense arrangement. Fig. 5b shows the light J-V curves of the best PSCs prepared from different solutions. The PSC prepared from the solution of 2:1 has a power conversion efficiency (PCE) of 7.48%, with a short circuit current density (J_{sc}) of 7.16 mA cm^{-2}, a fill factor (FF) of 74.07%, and an open-circuit voltage V_{oc} of 1.41 V. Whereas the best PSCs fabricated from the solution of 2:0 and 2:0.5 exhibit very low PCE of 0.99% and 3.73%, respectively. Other photovoltaic parameters from different PSCs are summarized in Table 1. This performance comparison shows the importance of enhancing the purity and coverage of $CsPbBr_3$ phase in active layer of solar cell. Fig. 5c is the steady-state output near the maximum power point of the best PSC of the 2:1 device. A steady photocurrent density of 5.65 mA cm^{-2} and a steady PCE of 6.44% were obtained at a bias voltage 1.14 V. It is noted that the steady PCE is slightly lower than the value extracted from J-V curve under the reverse scan. The deviation might come from the hysteresis behavior which is usually observed in common PSC devices [11,27–30] (Fig. S7). The IPCE spectrum of the optimized solar cell is recorded and shown in Fig. 5d. The device shows strong light absorption ability in the range of 300–~525 nm. The J_{sc} integrated from the IPCE spectra is 6.46 mA cm^{-2}, which is a little lower than that obtained from the *J-V* curve. This discrepancy might be related to the nonlinear properties of perovskite films [31]. It should be noted that a high V_{oc} of 1.5 V is achieved in a patch of PSCs prepared from the solution of 2:1. This value is one of the highest V_{oc} for the $CsPbBr_3$ solar cells based on unmodified configuration FTO/TiO_2/$CsPbBr_3$/Carbon [32]. Fig. 5f summarizes the distribution of PCE collected from a series of PSCs. The average PCE is 5.86% of all samples demonstrating that our two-steps method is a reliable way to prepare efficient $CsPbBr_3$ solar cells.

The air stability of solar cells is also investigated. Fig. 6 shows the normalized photovoltaic parameters of an unencapsulated PSC under the open-air condition (T ~30 °C RH ~45%). The result shows that the photovoltaic parameters, including V_{oc}, J_{sc}, FF and PCE, are still stable over 50 days. The best-performance PSC still shows a PCE of 6.81%, V_{oc} of 1.41 V, J_{sc} of 7.21 mA cm^{-2}, and FF of 67% when it is stored in ambient condition for 90 days (see Fig. S8). The superior stability of $CsPbBr_3$ solar cells makes it become a competitive candidate to the commercialization of PSCs.

4. Conclusion

In summary, we fabricate high-quality $CsPbBr_3$ films by using a facile two-step spin-coating method, in which CsBr is introduced into $PbBr_2$ solution in the first step. The pre-incorporated CsBr in $PbBr_2$ solution can shorten the fabrication period and simplify the preparation process in comparison with the traditional dipping and multi-step solution processing methods. The $CsPbBr_3$ films are used to fabricate solar cell

devices with a configuration of FTO/TiO_2/$CsPbBr_3$/Carbon. The optimized samples can achieve a power conversion efficiency of 7.48%, with high stability in air conditions. These results demonstrate the efficient and time-saving method for preparation of $CsPbBr_3$ films in this work has a promising application in various optoelectronic devices.

Declaration of competing interest

The authors declare that they have no known competing financial interests or personal relationships that could have appeared to influence the work reported in this paper.

Acknowledgements

This work was financially supported by National Natural Science Foundation of China (Grant No. 52202287 and 61974010) and Guangdong Basic and Applied Basic Research Foundation (Grant No. 2020A1515111052).

Appendix A. Supplementary data

Supplementary data to this article can be found online at https://doi.org/10.1016/j.ceramint.2023.03.279.

References

[1] J. Liang, C. Wang, Y. Wang, Z. Xu, Z. Lu, Y. Ma, H. Zhu, Y. Hu, C. Xiao, X. Yi, G. Zhu, H. Lv, L. Ma, T. Chen, Z. Tie, Z. Jin, J. Liu, All-inorganic perovskite solar cells, J. Am. Chem. Soc. 138 (2016) 15829–15832, https://doi.org/10.1021/jacs.6b10227.

[2] I. Poli, J. Baker, J. McGettrick, F.D. Rossi, S. Eslava, T. Watson, P.J. Cameron, Screen printed carbon $CsPbBr_3$ solar cells with high open-circuit photovoltage, J. Mater. Chem. 6 (2018) 18677–18686, https://doi.org/10.1039/C8TA07694D.

[3] X. Chang, W. Li, L. Zhu, H. Geng, S. Xiang, J. Liu, H. Chen, Carbon-based $CsPbBr_3$ perovskite solar cells: all-ambient process and high thermal stability, ACS Appl. Mater. Interfaces 8 (2016) 33649–33655, https://doi.org/10.1021/acsami.6b11393.

[4] G. Wang, W. Dong, A. Gurung, K. Chen, F. Wu, Q. He, R. Pathak, Q. Qiao, Improving photovoltaic performance of carbon-based $CsPbBr_3$ perovskitesolar cells by interfacial engineering using P3HT interlayer, J. Power Sources 432 (2019) 48–57, https://doi.org/10.1016/j.jpowsour.2019.05.075.

[5] M. Kulbak, D. Cahen, G. Hodes, How important is the organic part of lead halide perovskite photovoltaic cells? Efficient $CsPbBr_3$ perovskite solar cells, J. Phys. Chem. Lett. 6 (2015) 2452–2456, https://doi.org/10.1021/acs.jpclett.5b00968.

[6] M. Kulbak, S. Gupta, N. Kedem, I. Levine, T. Bendikov, G. Hodes, D. Cahen, Cesium enhances long-term stability of lead bromide perovskite-based solar cells, J. Phys. Chem. Lett. 7 (2016) 167–172, https://doi.org/10.1021/acs.jpclett. 5b02597.

[7] G. Wang, J. Bi, J. Chang, M. Lei, H. Zheng, Y. Yan, Bandgap tuning of a $CsPbBr_3$ perovskite with synergistically improved quality via Sn^{2+} doping for high-performance carbon-based inorganic perovskite solar cells, Inorg. Chem. Front. 9 (2022) 4359–4368, https://doi.org/10.1039/D2QI00802E.

[8] K.C. Tang, P. You, F. Yan, Highly stable all-Inorganic perovskite solar cells processed at low temperature, Sol. RRL 2 (2018), 1800075, https://doi.org/10.1002/solr.201800075.

[9] J. Feng, X. Han, H. Huang, Q. Meng, Z. Zhu, T. Yu, Z. Li, Z. Zou, Curing the fundamental issue of impurity phases in two-step solution-processed $CsPbBr_3$ perovskite films, Sci. Bull. 65 (2020) 726–737, https://doi.org/10.1016/j.scib.2020.01.025.

[10] J. Li, Z. Zhi, X. Han, T. Yu, Y. Xu, J. Feng, Z. Li, Z. Zou, Direct molecule substitution enabled rapid transformation of wet $PbBr_2$(DMF) precursor films to $CsPbBr_3$ perovskite, ACS Appl. Energy Mater. 4 (2021) 6414–6421, https://doi.org/10.1039/C9EE01 479A.

[11] J. Ryu, S. Yoon, S. Lee, D. Lee, B. Parida, H.W. Kwak, D.W. Kang, Improving photovoltaic performance of $CsPbBr_3$ perovskite solar cells by a solvent-assisted rinsing step, Electrochim. Acta 368 (2021), 137539, https://doi.org/10.1016/j.electacta.2020.137539.

[12] J. Duan, Y. Zhao, B. He, Q. Tang, High-purity inorganic perovskite films for solar cells with 9.72% efficiency, Angew. Chem. Int. Ed. 57 (2018) 3849–3853, https://doi.org/10.1002/anie.201800019.

[13] P. Teng, X. Han, J. Li, Y. Xu, L. Kang, Y. Wang, Y. Yang, T. Yu, Elegant face-down liquid-space-restricted deposition of $CsPbBr_3$ films for efficient carbon-based all-Inorganic planar perovskite solar cells, ACS Appl. Mater. Interfaces 10 (2018) 9541–9546, https://doi.org/10.1021/acsami.8b00358.

[14] Q. Meng, J. Feng, H. Huang, X. Han, Z. Zhu, T. Yu, Z. Li, Z. Zou, Simultaneous optimization of phase and morphology of $CsPbBr_3$ films via controllable Ostwald ripening by ethylene glycol monomethylether/isopropanol bi-solvent engineering, Adv. Eng. Mater. 22 (2020), 2000162, https://doi.org/10.1002/adem.202000162.

[15] J. Chen, W. Qiu, C. Huang, L. Wu, C. Liu, Q. Tian, Z. Peng, J. Chen, A novel solvent for multistep solution-processed planar $CsPbBr_3$ perovskite solar cells using In_2S_3 as electron transport layer, Energy Technol. 10 (2020), 2200054, https://doi.org/10.1002/ente.202200054.

[16] X. Cao, G. Zhang, L. Jiang, Y. Cai, Y. Gao, W. Yang, X. He, Q. Zeng, G. Xing, Y. Jia, J.Q. Wei, Water, a green solvent for fabrication of high quality $CsPbBr_3$ films for efficient solar cells, ACS Appl. Mater. Interfaces 12 (2020) 5925–5931, https://doi.org/10.1021/acsami.9b20376.

[17] E. Belarbi, M. Vallés-Pelarda, B.C. Hame, R.S. Sanchez, E.M. Barea, H.M. Meherzi, I.M. Seró, Transformation of PbI_2, $PbBr_2$ and $PbCl_2$ salts into $MAPbBr_3$ perovskite by halide exchange as an effective method for recombination reduction, Phys. Chem. Chem. Phys. 19 (2017) 10913–10921, https://doi.org/10.1039/C7CP01192J.

[18] J. Liu, L. Zhu, S. Xiang, Y. Wei, M. Xie, H. Liu, W. Li, H. Chen, Growing high-quality $CsPbBr_3$ by using porous $CsPb_2Br_5$ as an intermediate: a promising light absorber in carbon-based perovskite solar cells, Sustain. Energy Fuels 3 (2019) 184–194, https://doi.org/10.1039/C8SE00442K.

[19] T. Liu, Q. Hu, J. Wu, K. Chen, L. Zhao, F. Liu, C. Wang, H. Lu, S. Jia, T. Russell, R. Zhu, Q. Gong, Mesoporous PbI_2 scaffold for high-performance planar heterojunction perovskite solar cells, Adv. Energy Mater. 6 (2016), 1501890, https://doi.org/10.1002/aenm.201501890.

[20] X. Han, X. Wang, J. Feng, H. Huang, Z. Zhu, T. Yu, Z. Li, Z. Zou, Carrier mobility enhancement in (121)-oriented $CsPbBr_3$ perovskite films induced by the microstructure tailoring of $PbBr_2$ precursor films, ACS Appl. Electron. Mater. 3 (2021) 373–384, https://doi.org/10.1021/acsaelm.0c00909.

[21] X. Liu, X. Tan, Z. Liu, H. Ye, B. Sun, T. Shi, Z. Tang, G. Liao, Boosting the efficiency of carbon-based planar $CsPbBr_3$ perovskite solar cells by a modified multistep spin-coating technique and interface engineering, Nano Energy 56 (2019) 184–195, https://doi.org/10.1016/j.nanoen.2018.11.053.

[22] J. Seo, J.H. Noh, S.I. Seok, Rational strategies for efficient perovskite solar cells, Acc. Chem. Res. 49 (2016) 562–572, https://doi.org/10.1021/acs.accounts.5b00444.

[23] W. Zhu, Z. Zhang, W. Chai, D. Chen, H. Xi, J. Chang, J. Zhang, C. Zhang, Y. Hao, Benign pinholes in $CsPbIBr_2$ absorber film enable efficient carbon-based, all-inorganic perovskite solar cells, ACS Appl. Energy Mater. 2 (2019) 5254–5262, https://doi.org/10.1021/acsaem.9b00944.

[24] Y. Zhao, K. Zhu, Organic–inorganic hybrid lead halide perovskites for optoelectronic and electronic applications, Chem. Soc. Rev. 45 (2016) 655–689, https://doi.org/10.1039/C4CS00458B.

[25] J. Duan, Y. Zhao, B. He, Q. Tang, Simplified perovskite solar cell with 4.1% efficiency employing inorganic $CsPbBr_3$ as light absorber, Small 14 (2018), 1704443, https://doi.org/10.1002/smll.201704443.

[26] J. Duan, T. Hu, Y. Zhao, B. He, Q. Tang, Carbon electrode tailored all-inorganic perovskite solar cells to harvest solar and water-stream energies, Angew. Chem. Int. Ed. 57 (2018) 5746–5749, https://doi.org/10.1002/anie.201801837.

[27] Y. Pei, H. Guo, Z. Hu, J. Zhang, Y. Zhu, $BiBr_3$ as an additive in $CsPbBr_3$ for carbon-based all-inorganic perovskite solar cell, J. Alloys Compd. 853 (2020), 155283, https://doi.org/10.1016/j.jallcom.2020.155283.

[28] T. Xiang, Y. Zhang, H. Wu, J. Li, L. Yang, K. Wang, J. Xia, Z. Deng, J. Xiao, W. Li, Z. Ku, F. Huang, J. Zhong, Y. Peng, Y.B. Cheng, Universal defects elimination for high performance thermally evaporated $CsPbBr_3$ perovskite solar cells, Sol. Energy Mater. Sol. Cells 206 (2020), 110317, https://doi.org/10.1016/j.solmat.2019.110317.

[29] O. Almora, I. Zarazua, E.M. Marza, I.M. Sero, J. Bisquert, G.G. Belmonte, Capacitive dark currents, hysteresis, and electrode polarization in lead halide perovskite solar cells, J. Phys. Chem. Lett. 6 (2015) 1645–1652, https://doi.org/10.1021/acs.jpclett.5b00480.

[30] J. Yan, S. Hou, X. Li, J. Dong, L. Zou, M. Yang, J. Xing, H. Liu, H. Hao, Preparation of highly efficient and stable $CsPbBr_3$ perovskite solar cells based on an anti-solvent rinsing strategy, Sol. Energy Mater. Sol. Cells 234 (2022), 111420, https://doi.org/10.1016/j.solmat.2021.111420.

[31] M. Saliba, L. Etgar, Current density mismatch in perovskite solar cells, ACS Energy Lett. 5 (2020) 2886–2888, https://doi.org/10.1021/acsenergylett.0c01642.

[32] X. Cao, G. Zhang, L. Jiang, Y. Cai, Y. Wang, X. He, Q. Zeng, J. Chen, Y. Jia, J. Wei, Achieving environment-friendly production of $CsPbBr_3$ films for efficient solar cells via precursor engineering, Green Chem. 23 (2021) 2104–2112, https://doi.org/10.1039/D1GC00106J.